BABAR-PROC-00/11
SLAC-PUB-8622

First Year of the *BABAR* Experiment Data Taking

Marc Verderi
Laboratoire de Physique Nucléaire des Hautes Energies
Ecole Polytechnique
91128 Palaiseau, FRANCE
(for the *BABAR* Collaboration.)

Abstract

The *BABAR* experiment at the PEP-II asymmetric B Factory observed its first hadronic events on the 26^{th} of May 1999. We present the progress made so far on the data taking, the *BABAR* detector performances and the physics analyses.

Contribued to the Proceedings of the XX^{th} Physics in Collision,
6/29/2000—7/1/2000, Lisbon, Portugal

Stanford Linear Accelerator Center, Stanford University, Stanford, CA 94309

Work supported in part by Department of Energy contract DE-AC03-76SF00515.

1 Introduction

The primary goal of the *BABAR* experiment at PEP-II is to over-constraint the unitarity triangle. The sides of this triangle can be measured through non-*CP* violating physics, while its angles are accessible through *CP*-violating processes [1]. The first measurable angle will be $\sin 2\beta$ with the so called "golden plated" channel $B^0 \to J/\psi K^0_S$. Because of the variety of processes to be studied, *BABAR* has been designed as a general HEP detector [2] and can also be useful for non-CKM matrix physics.

The *CP* violation is studied through time-dependant *CP* asymmetries:

$$A_{CP}(t) = \frac{\Gamma(B^0 \to f_{CP}) - \Gamma(\overline{B}^0 \to f_{CP})}{\Gamma(B^0 \to f_{CP}) + \Gamma(\overline{B}^0 \to f_{CP})} = A_{CP}.\sin(\Delta m_B \cdot t) \tag{1}$$

where f_{CP} denotes a particular *CP* eigenstate final state and Δm_B the mass difference between the two neutral B mass eigenstates. In the Standard Model, this A_{CP} term for the $B^0 \to J/\psi K^0_S$ channel is directly $\sin 2\beta$.

The measurement of $A_{CP}(t)$ relies on the determination of two ingredients: the B meson decay time t and the flavor B^0 or $\overline{B}^0$ of this B meson at $t = 0$.

The principle adopted by asymmetric B Factories is to produce $B^0\overline{B}^0$ pairs through the asymmetric e^+e^-collisions, $e^+e^- \to \Upsilon(4S) \to B^0\overline{B}^0$, so that the $B^0\overline{B}^0$ system formed is boosted.

Because the $\Upsilon(4S)$ is $J^{PC} = 1^{--}$, the $B^0\overline{B}^0$ system is in an antisymmetric state. That garanties that at all times, the two Bs will have opposite flavors. Once one of the B decays it is possible to infer its flavor by measuring its decay products. The sign of a lepton present in the decay products, taking care if this lepton is direct or indirect, can be used, as well as kaon sign, for example. This flavor determination is called the "tagging". Thanks to the antisymmetry of the $B^0\overline{B}^0$ system, we know that the other B meson, has the opposite flavor at that time, which define $t = 0$ in 1.

The measurement of the distance Δz between the two decay vertices, which is about 260 μm on average at PEP-II, provides the measurement of the $B \to f_{CP}$ decay time t, the second ingredient of equation 1, through $t = \Delta z/\beta\gamma c$.

Beyond the need of an asymmetric machine, other requirements have to be met: the B vertices reconstruction implies an excellent tracking and vertexing capability. Because $B \to f_{CP}$ modes have low branching ratios, typically at the 5×10^{-5} level, a high luminosity is needed. The tagging requires good lepton and kaon identification.

Those requirements have driven the PEP-II and *BABAR* designs.

2 The PEP-II machine

The PEP-II machine reuses the existing Linac injector part (see figure 1). The positrons circulate in the Low Energy Ring (LER) which was also an existing part. The High Energy Ring (HER) has been specially built.

The beam energies and center of mass boost are:

$$e^-(9\,\mathrm{GeV}) \otimes \mathrm{e}^+(3.1\,\mathrm{GeV}) \Rightarrow \beta\gamma \sim 0.56$$

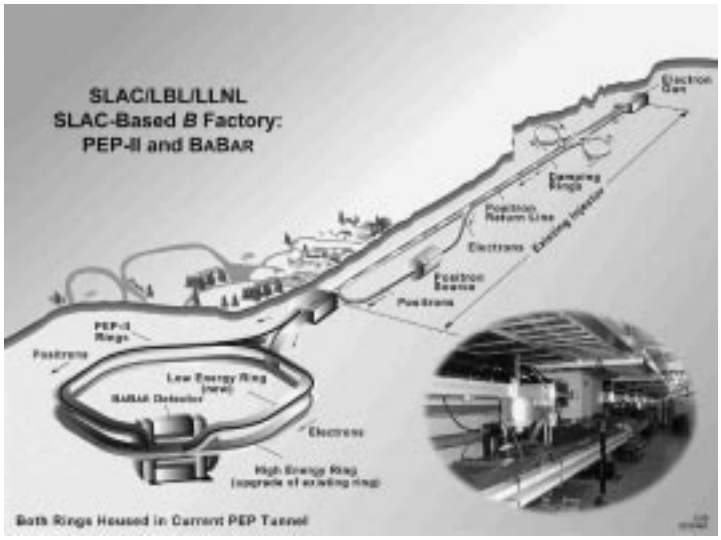

Figure 1: The PEP-II storage rings.

Table 1: PEP-II performances

	design	achieved	typical
Luminosity ($\mathrm{cm^{-2}s^{-1}}$)	3×10^{33}	2.2×10^{33}	$1.9 - 2.1 \times 10^{33}$
LER current (A)	2.14	1.7	1.1
LER lifetime	$4h$@$2A$	$3.5h$@$1A$	$3h$@$1A$
HER current (A)	0.75	0.92	0.65
HER lifetime	$4h$@$1A$	$11h$@$0.9A$	$9h$@$0.65A$
#bunches(HER/LER)	1658	1658	829

Table 1 shows the designed, achieved and typical values of the PEP-II parameters. The designed values have all been or are close to be achieved, and are also close to the typical ones.

With such high currents, one may worry about the level of radiation delivered to the *BABAR* subsystems. Figure 2(left) shows the daily radiation dose delivered by the HER at two positions in the Silicon Vertex Tracker, in the horizontal (top) and vertical (bottom) planes over the past year. Limits for half and full design lifetimes are shown on this figure. Those dose rates can be turned into dose budgets which can be allowed. These dose budgets are drawn on figure 2(right), showing that they are not overspent.

The *BABAR*/PEP-II "Factory Mode" can be illustrated with a few numbers: the daily recorded luminosity is at present in the 120 to 140 $\mathrm{pb^{-1}}$ range, PEP-II delivers long duration fills, the record being 22 hours, and the *BABAR* data taking efficiency is typically 95 to 97%.

The accumulated data sample at the time of this conference is about $11\,\mathrm{fb^{-1}}$.

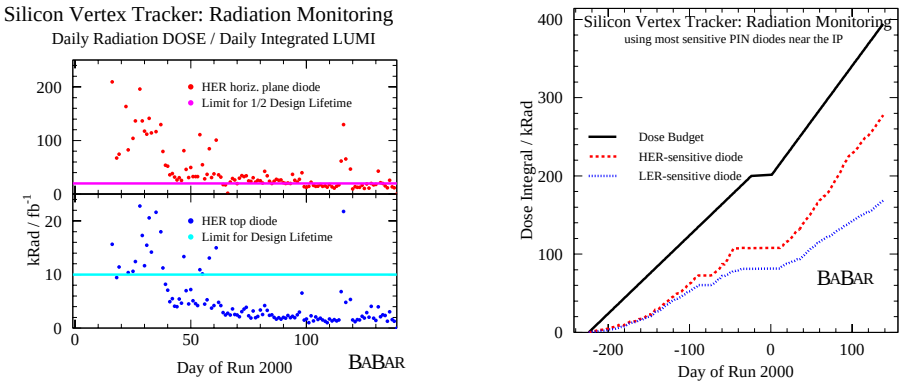

Figure 2: Silicon Vertex Tracker daily delivered dose (left) and dose budget (right).

3 *BABAR* detector highlights

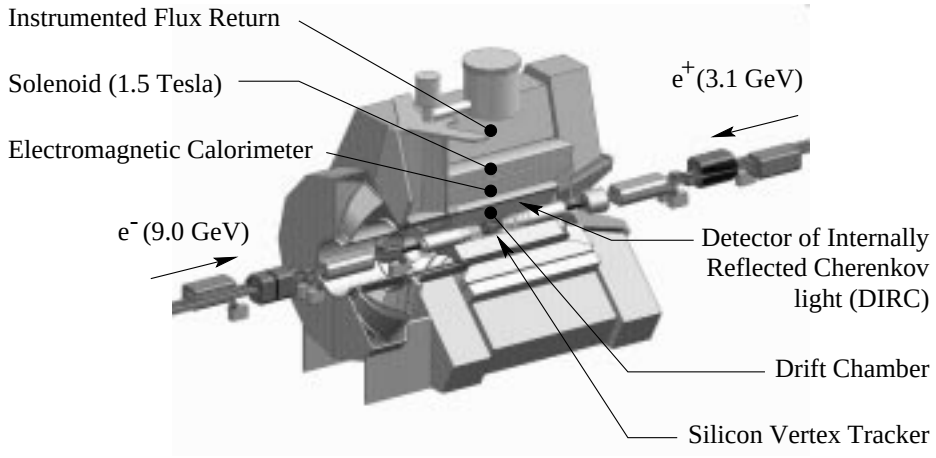

Figure 3: *BABAR* detector layout.

Figure 3 shows the *BABAR* layout. Electrons enter from the front *BABAR* side. The center of mass boost induced the asymmetric design with an interaction point displaced from the geometrical center in the backward direction.

3.1 Silicon Vertex Tracker (SVT)

The SVT is made of 5 layers, double side silicon. It is built in radiation-hard technologies, allowing up to 2 Mrad dose. The SVT extends from 3.3 cm to 14.6 cm in radius. The three inner layers are dedicated to measurement of the impact parameter d_0 and the angle of the tracks. The two outer layers allow track pattern recognition of slow particles, which makes the Silicon Vertex "Tracker" capable of *standalone tracking*. The z and d_0 resolutions have been measured using muons of transverse momentum above 2 GeVto be better than 40 μm.

The alignment of the SVT is an important issue. The relative SVT/Drift Chamber diurnal motions are measured to be as large as 70 μm. The alignment corrections are computed on a run by run basis as part of the reconstruction, in a procedure called the *"rolling calibration"*.

3.2 Drift Chamber (DCH)

The Drift Chamber is made of $\sim$ 7000 drift cells with hexagonal field wire pattern. It is filled with a 80/20 % He/C_4H_{10} gas mixture in order to minimize the multiple scattering.

The single hit resolution measured with tracks above 1 GeV is approximately 125 μm, better than the design value ($\sim$ 140 μm). The dE/dx resolution is about 7.5 % for Bhabha events (the design value being 7 %). This dE/dx resolution allows a 2σ K/π separation up to 700 MeV/c.

3.3 Detector of Internally Reflected Cherenkov light (DIRC)

The DIRC is the main particle identification device of *BABAR*. It provides identification of particles above 500 MeV/c. The radiator part is made of quartz bars arranged in 12 sectors. The Cherenkov light produced by charged particles in the quartz is transported by internal reflections down to the Stand Of Box, a water filled expansion, visible on figure 3 at the rear of *BABAR*. An array of 10 752 photo-multipliers reads the image formed by the Cherenkov light.

The Cherenkov angle resolution per track is $\sigma(\theta_C) = 3.0$ mrad, for a targeted resolution of 2.0 mrad. This resolution allows presently a 2.1σ K/π separation at 4 GeV.

Figure 4 shows a $D^0 \to K^{\pm}\pi^{\mp}$ signal peaks, without (left) and with (right) kaon identification from the DIRC.

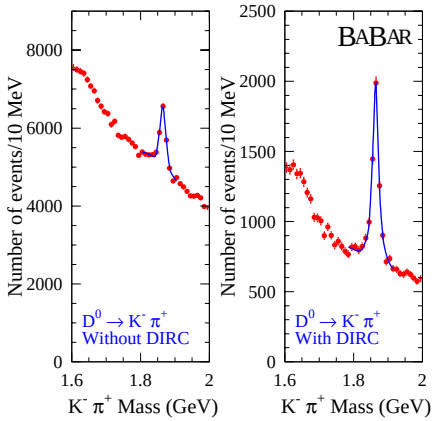

Figure 4: $D^0 \to K^{\pm}\pi^{\mp}$ signal peaks where the $K^{\pm}$ is inside the DIRC acceptance, without (left) and with (right) kaon indentification ($\theta_C(K^{\pm})$ required to be within 2σ of the kaon hypothesis). This allows a background rejection of a factor of about 5. (Note that the remaining background contains true kaons.)

3.4 Electromagnetic Calorimeter (EMC)

The Electromagnetic Calorimeter consists of 6580 CsI(Tl) crystals. It is made of a barrel and a forward end-cap. The resolution achieved on $\pi^0 \to \gamma\gamma$ signal mass peak, requiring $E_\gamma > 30$ MeV, is 6.9 MeV, in good agreement with Monte Carlo expectation.

Electron identification is performed in the EMC. The electron detection efficiency $\epsilon(e^{\pm})$ is typically 92 % above 1 GeV/c. The pion misidentification probability $\epsilon(\pi^{\pm})$ is measured below 2 GeV/c on a sample of pions from $K^0_s \to \pi^+\pi^-$ decays and is found to be about 0.3 %.

3.5 Instrumented Flux Return (IFR)

The Instrumented Flux Return is made of bakelite-based resistive plate chambers sandwiched between iron plates. It provides muon identification above 500 MeV/c and K^0_L detection.

Beetwen 1.5 GeV/c and 3 GeV/c the muon identification efficiency is about 75 % and the pion misidentification probability 2.4 %.

4 Physics status in *BABAR*

Lot of activity is going on within *BABAR* both on *CP* and non-*CP* physics. The analyses are in "validation" phase, which means that the current concerns are the understanding and the control of the mass spectra resolutions, yields, and also the control of more complex algorithm like the tagging one.

The idea here is not to make an exhaustive status of the analysis but rather try to give a flavor of the current effort and point out aspects relevant for *CP* measurement.

4.1 $B \to J/\psi\, K$ and $B \to \psi(2S)K$

Figure 5 shows the di-muon(left) and di-electron(right) invariant mass spectra. The radiative tail due to bremsstrahlung is clearly visible on the di-electron mass peak.

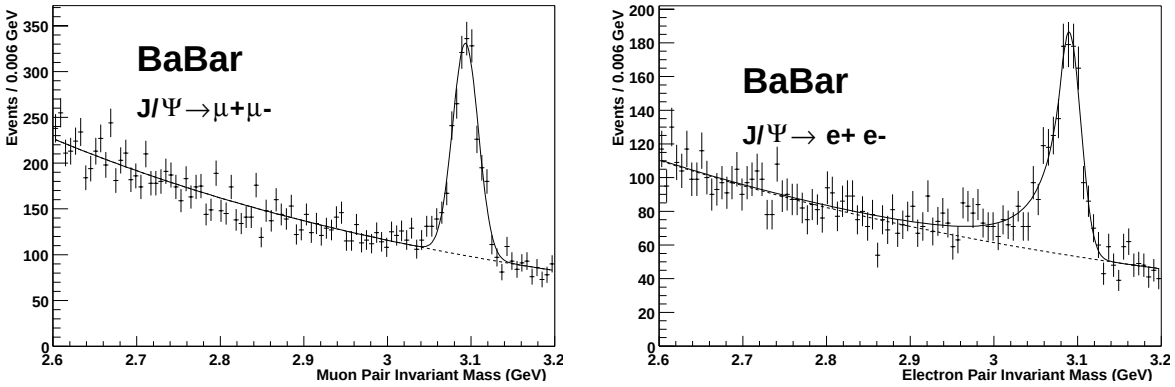

Figure 5: J/ψ candidates in the di-muon (left) and di-electron (right) channels.

Those spectra are obtained from a ~ 2 fb^{-1}data sample. The numbers of J/ψ candidates in both peaks are compatible with expectations. The mass resolution of the $J/\psi \to \mu^+\mu^-$ signal peak is ~ 15 MeV/c^2. Thanks to the "rolling calibration" procedure mentionned above, this resolution is improving now and is close to 11 MeV/c^2.

Figure 6 shows the $B^0 \to J/\psi\, K^0_S$ (left) and $B^+ \to J/\psi\, K^+$ (right) candidates from a ~ 2 fb^{-1}data sample. The former are used in the *CP* violation measurement. The upper plots show

the signals in the "ΔE" versus the "beam constrained mass" M_B plan defined as follows:

$$M_B = \sqrt{{E^*_{Beam}}^2 - {p^*_B}^2} \quad (2)$$
$$\Delta E = E^*_B - E^*_{Beam} \quad (3)$$

where all quantities are expressed in the $\Upsilon(4S)$ center of mass, E^*_{Beam} being the beam energy, p^*_B and E^*_B being the measured B candidate momentum and energy respectively.

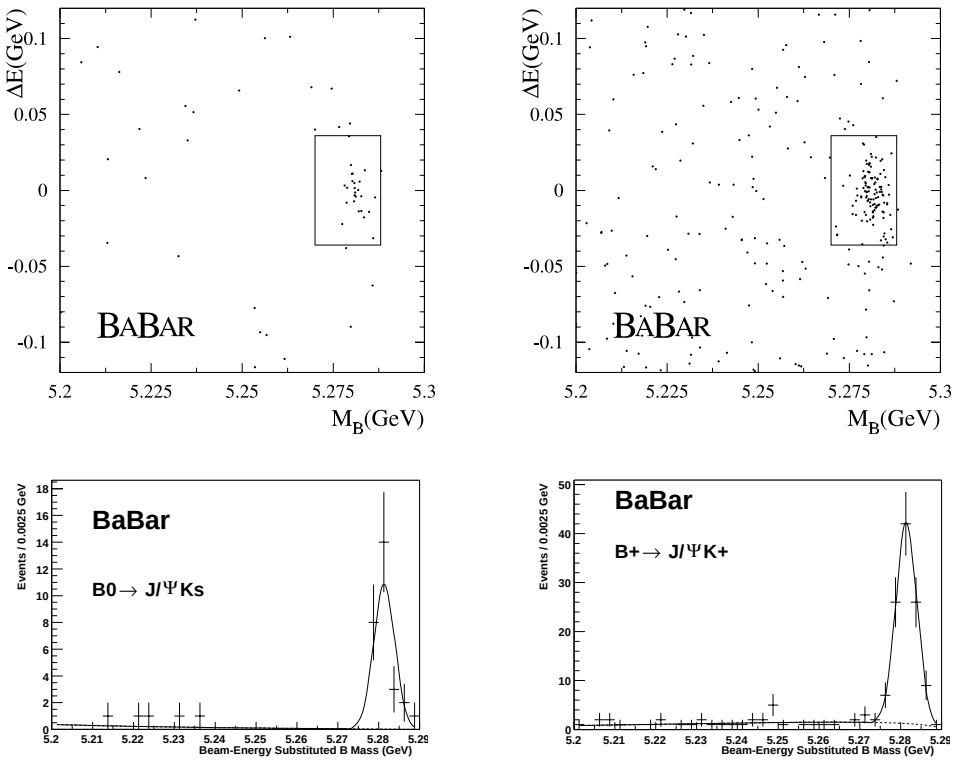

Figure 6: $B^0 \to J/\psi K^0_S$ (left) and $B^+ \to J/\psi K^+$ (right) candidates from a ~ 2 fb^{-1}data sample. Upper plots show the candidates in the ΔE versus the "beam constrained mass" M_B defined in the text. The squares on the top plots represent the "signal region" and correspond to roughly $\pm$ 3 σ on ΔE and M_B. Bottom plots are projections of M_B within a $\pm 3\sigma$ band in ΔE.

The number of events observed in the signal regions (see figure 6) are 28 and 109 in the $B^0 \to J/\psi K^0_S$ and $B^+ \to J/\psi K^+$ channels respectively and are compatible with expectations. The M_B projections (see figure 6) show that both signals are very clean.

$B^+ \to J/\psi K^+$ events are also used to check on the data the reconstruction of Δz which enters the *CP* asymmetry (equation 1) through $t = \Delta z/\beta\gamma c$. The resolution is measured to be $\sigma(\Delta z) \sim 100\,\mu$m (with a 20 % additional component of $\sim 320\,\mu$m of σ) in good agreement with Monte Carlo expectation.

Other channels interesting for the *CP* violation measurement are investigated. Figure 7(bottom) shows for example the $B \to \psi(2S)K$ candidates. The related $\psi(2S)$ charmonia are reconstructed

in the $\psi(2S)\to l^+l^-$ and $\psi(2S)\to J/\psi\,\pi^+\pi^-$ channels (figure 7(up)). Six events are observed in the signal box of the *CP* channel $B^0 \to \psi(2S)K^0_S$ with a 0.5 estimated background and a 19 events yield is found in the $B^+ \to \psi(2S)K^+$ channel.

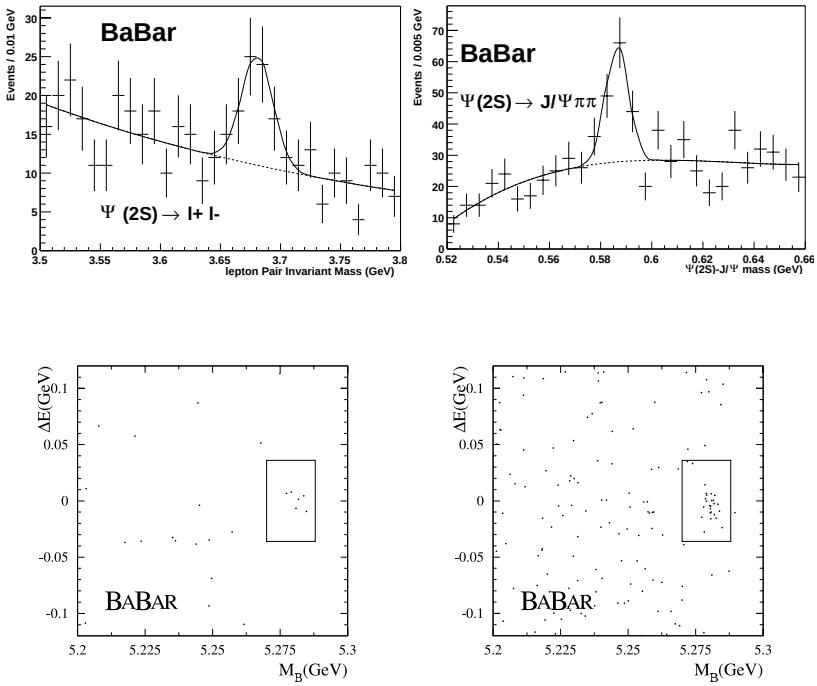

Figure 7: Top: $\psi(2S)\to l^+l^-$ (left) and $\psi(2S)\to J/\psi\,\pi^+\pi^-$ (right) candidates. The latter are displayed making the difference of masses between the $\psi(2S)$ and J/ψ candidates. Bottom: $B^0 \to \psi(2S)K^0_S$ candidates (left), $B^+ \to \psi(2S)K^+$ candidates (right) formed using above $\psi(2S)$.

4.2 B to open charm and CP engineering

B decays to charm provide larges samples of clean reconstructed Bs in semileptonic and hadronic modes. Beyond the intrisic physics interest, B to open charm allow powerful CP engineering studies. We expose here the important issue of the control of the tagging algorithm and present the strategy adopted by *BABAR* to perform this control.

The tagging algorithm is characterized by two quantities: the tagging efficiency ϵ_{tag} which is the fraction of Bs for which the tagging algorithm gives an answer, and the mis-tag fraction w which is the wrong $B^0/\overline{B}^0$ assignment probability.

The mis-tag fraction is a key parameter because it induces two effects:

- It increases the uncertainty σ on sin2β:

$$\sigma \to \frac{\sigma}{\sqrt{\epsilon_{tag}(1-2w)^2}} = \frac{\sigma}{\sqrt{\epsilon_{tag}^{effective}}}$$

  (Note that $\epsilon_{tag}^{effective}$ is typically of the order of 20 to 30 %.)

- But moreover it induces a *bias* on the asymmetry:

$$A_{CP} \propto \frac{A_{CP}^{observed}}{(1-2w)}$$

Since the tagging algorithm exploits mainly all the detector subsystems for leptons and kaons identification, many possible sources of systematics errors are faced at once.

The strategy adopted by *BABAR* is to perform a global control on the data themselves.

Samples of neutral B mesons with known B^0 or $\overline{B}^0$ flavor are reconstructed. The tagging algorithm is applied on the recoil tracks, as in a *CP* analysis. The sample where both B mesons are found to have the same flavor is retained. Two contributions form this sample: one from B^0-$\overline{B}^0$ mixing events and the other one from non-mixing events, but with a wrong $B^0/\overline{B}^0$ assignment from the tagging algorithm. Each contribution has a well known time distribution, controled by the Δm_B parameter.

A fit on the time distribution on this "same flavor events sample" allows to separate those two contributions and thus to extract the w parameter. Moreover, by extracting w on a given time window, using the knowledge on Δm_B, the w value obtained can be re-used outside this time window to measure back Δm_B as a cross-check.

This study can be done using various B to open charm channels. We illustrate here the statistical power of this method with the $B_d^0 \to D^{*-} l^+ \nu$ channel.

The $B_d^0 \to D^{*-} l^+ \nu$ events are reconstructed within three channels according to the D^0 decay from the $D^* \to D^0 \pi_{soft}$ decay:

$$\begin{array}{lcl} D^0 & \to & K\,\pi \\ D^0 & \to & K\,\rho(\pi\pi^0) \\ D^0 & \to & K\,3\pi \end{array}$$

The selection is based on a missing mass to be compatible with a neutrino mass, which translates into the constraint $-1 < \cos(\theta_{B-D^*l}) < +1$ and the difference of mass Δm between the D^* and the D^0 candidates: $\Delta m = m(K\pi[\pi][\pi]\pi_{soft}) - m(K\pi[\pi][\pi])$ to be compatible with the nominal difference of masses.

The three B samples from $D^0 \to K\pi$, $D^0 \to K\pi\pi^0$ and $D^0 \to K3\pi$ channels are shown on figure 8. The luminosity used is ~ 3.3 fb^{-1}. The total number of reconstructed events is about 2 600. The Δm_B value retrieved in the cross-check procedure explained above is in good agreement with the world average, making the w value trustable. Thanks to this high number of reconstructed events, the effect of the incertainty on the measured w value on the sin2β measurement is kept smaller than the statistical error on sin2β.

4.3 Dilepton mixing

This analysis is quite similar to the previous one except that only leptons are considered to infer the B flavor. It measures the asymmetry between "same sign" and "opposite sign" di-lepton events:

$$A(\Delta t) = \frac{N_B(l^\pm l^\mp) - N_B(l^\pm l^\pm)}{N_B(l^\pm l^\mp) + N_B(l^\pm l^\pm)}$$

The today observed asymmetry is shown on figure 9. This analysis should provide a competitive measurement on Δm_B.

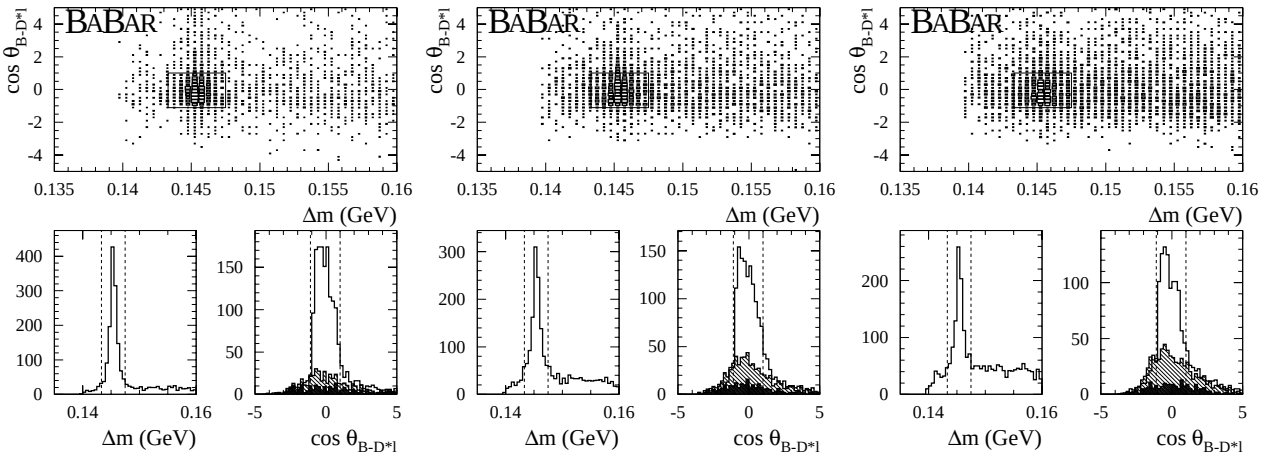

Figure 8: $B^0_d \to D^{*-} l^+ \nu$ candidates. The left, middle and right plots are the $D^0 \to K\pi$, $D^0 \to K\pi\pi^0$ and $D^0 \to K3\pi$ samples respectively. The samples are shown in the $\cos(\theta_{B-D^*l})$ versus Δm plans defined in the text. The 1D projections are also shown.

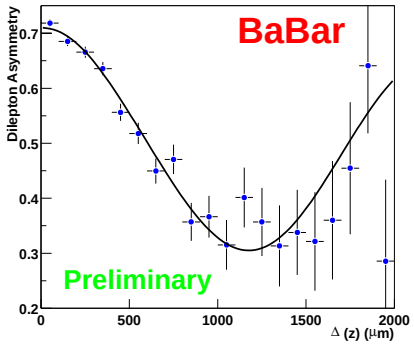

Figure 9: Dilepton $l^{\pm}l^{\mp}$ - $l^{\pm}l^{\pm}$ asymmetry.

5 Conclusion

BABAR and PEP-II have had a terrific start. 11 fb^{-1} have been recorded since the end of May 1999 and the *BABAR* detector performances are close to the design values.

The ingredients necessary to the sin2β measurement are under control: the "golden plated" channel $B^0 \to J/\psi K^0_S$ is reconstructed with low background and understood yield. The Δz measurement and the tagging algorithm are controled on the data themselves.

The *BABAR*/PEP-II short and medium term plans are to run up to the end of October, with an expected collected data sample larger than 20 fb^{-1} and then to run at the designed luminosity $3 \times 10^{33}\,\mathrm{cm}^{-2}\mathrm{s}^{-1}$, which should allow *BABAR* to collect 30 fb^{-1} in one year.

6 Acknowledgments

We are grateful for the contributions of our PEP-II colleagues in achieving the excellent luminosity and machine conditions that have made this work possible. We acknowledge support from the Natural Sciences and Engineering Research Council (Canada), Institute of High Energy Physics (China), Commissariat à l'Energie Atomique and Institut National de Physique Nucléaire et de Physique des Particules (France), Bundesministerium für Bildung und Forschung (Germany), Istituto Nazionale di Fisica Nucleare (Italy), The Research Council of Norway, Ministry of Science and Technology of the Russian Federation, Particle Physics and Astronomy Research Council (United Kingdom), the Department of Energy (US), and the National Science Foundation (US). In addition, individual support has been received from the Swiss National Foundation, the A. P. Sloan Foundation, the Research Corporation, and the Alexander von Humboldt Foundation. The visiting groups wish to thank SLAC for the support and kind hospitality extended to them.

References

[1] The *BABAR* Physics Book: Physics at an Asymmetric B Factory, *BABAR* Collaboration (P.F. Harrison, ed. *et al.*, SLAC-R-504, October 1998.

[2] *BABAR* Collaboration, *BABAR* Technical Design Report, SLAC-R-95-457, March 1995.